Diffraction Effects in Hydrophone Measurements

Albert Goldstein, *Senior Member, IEEE*, Darshan R. Gandhi, and William D. O'Brien, Jr., *Fellow, IEEE*

***Abstract*—Theoretical and experimental methodology are presented for accurately determining the effective radii of unfocused, circular plane piston transducers as well as using tone burst hydrophone measurements to verify steady-state theoretical calculations. Experiments using two specially fabricated unfocused, composite piezoelectric transducers demonstrate the validity of the methodology. For spherically focused circular transducers, a simple model is used to estimate the transient diffraction encountered in co-axial flat hydrophone measurements.**

I. Introduction

Several basic objectives in ultrasound physics are: the accurate measurement of transducer acoustic parameters such as the unfocused, circular plane piston "effective" radius, and the accurate experimental verification of steady-state theoretical calculations. Both require measurements of "point" pressure. However, the coherence of the transmitted radiation, the finite hydrophone diameter, and the experimental geometry lead to diffraction effects which cause experimental measurements to deviate from ideal "point" values.

In this work we show how to use hydrophone measurements, with suitable corrections, to accomplish the above two goals. In particular: a methodology is demonstrated for correcting axial hydrophone measurements of pressure maxima and minima to axial "point" pressure maxima and minima for calculating the flat, circular plane piston effective radius; and the proper manner of performing tone burst experimental measurements for verification of steady-state theoretical calculations for unfocused transducers is demonstrated. And a simple geometric model is presented for estimating the transient diffraction duration for hydrophone measurements of spherically focused circular piston transducers.

II. Unfocused Circular Piston

Diffraction effects due to finite transducer and hydrophone sizes and measurement geometry must be properly taken into account. To do this, a diffraction correction D is typically used [1]. The diffraction correction D is the ratio of the spatially averaged acoustic pressure received at the hydrophone front face from the baffled circular transmitter to a plane wave with the same initial pressure emanating from the full infinite plane of the transmitter front face. Because the denominator of this fraction is essentially a constant, D is proportional to the hydrophone received signal.

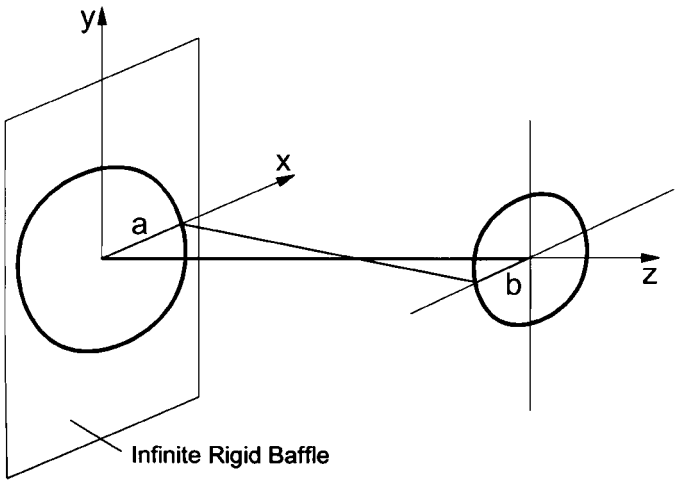

Fig. 1. Co-Axial transducer geometry with transmitter of radius a and receiver of radius b. The shortest acoustic path between the two transducers is between their centers, and the longest acoustic path is from opposite points on their edges as shown.

Fig. 1 illustrates the typical co-axial measurement geometry for a flat, circular piston transmitting transducer and a flat, circular piston receiving hydrophone with radii a and b, respectively. The D is a function of the positions, orientations, shapes, and sizes of the front face of both transducers.

Approximate and exact expressions for D exist that can be used to calculate the effect of hydrophone radius on measurements of the axial pressure of unfocused, circular piston transducers. An approximate expression was derived by Khimunin [2]:

$$D = 1 - \frac{2\sqrt{z^2+a^2}}{kab} J_1\left(\frac{kab}{\sqrt{z^2+a^2}}\right) \times \exp\left[-ik\left(\sqrt{z^2+a^2}-z\right)\right] \quad (1)$$

which is valid under the conditions $b/a \ll 1$, $ab/z^2 \ll 1$ and $a^2/\lambda \ll z^3/b^2$, where z is the axial distance from the transducer front face and λ is the acoustic wavelength in the propagation medium.

An exact theoretical expression for D was derived by Beissner [3] with $\gamma \equiv b/a$.

Manuscript received May 1, 1997; accepted February 4, 1998.

A. Goldstein is with the Department of Radiology, Detroit Receiving Hospital, Detroit, MI 48201 (e-mail: agoldste@med.wayne.edu).

D. R. Gandhi is with Motorola Inc., Rolling Meadows, IL 60008.

W. D. O'Brien, Jr. is with the Department of Electrical and Computer Engineering, Bioacoustics Research Laboratory, UIUC, Urbana, IL 61801.

For $\gamma \leq 1$:

$$D = e^{-jkz} - \frac{2}{\pi\gamma^2} \int_{1-\gamma}^{1+\gamma} \sqrt{1 - \left(\frac{1-\gamma^2+\xi^2}{2\xi}\right)^2} \times \exp\left[-jka\sqrt{\xi^2 + \left(\frac{z}{a}\right)^2}\right] d\xi. \quad (2)$$

For $\gamma \geq 1$:

$$D = \frac{e^{-jkz}}{\gamma^2} - \frac{2}{\pi} \int_{1-1/\gamma}^{1+1/\gamma} \sqrt{1 - \left(\frac{1-\gamma^{-2}+\xi^2}{2\xi}\right)^2} \times \exp\left[-jka\sqrt{(\gamma\xi)^2 + \left(\frac{z}{a}\right)^2}\right] d\xi. \quad (3)$$

For $\gamma = 1$, (2) and (3) are equal and give results identical with other calculations [1] for this specific case.

The approximate formula demonstrates very good agreement with the $\gamma \leq 1$ exact expression in the range of very small γ. It is faster in numerical computations, but the exact formulae are more accurate in all circumstances. Due to the availability and ease of use of numerical integration software for PCs, the exact formulae will be used here.

Comparison of calculations of D using (2) and (3) for reciprocal values of γ (exchanging the transmitter and receiver functions in Fig. 1) reveals a pseudo-reciprocity. The relative variation of D with z is identical, but the absolute magnitude of D differs. When $\gamma \to 0$, the spatial form of the axial point pressure of a flat, unfocused circular piston [4] is found with D varying between 0 and 2 [Fig. 2 (a)]. When $\gamma \to \infty$, the same spatial variation of D is found, but the magnitude of D goes to zero.

The cause of this observed pseudo-reciprocity is the form of the definition of D. The spatially averaged pressure caused by the infinite plane wave in the denominator will be constant and independent of γ. For small γ, the receiving transducer is getting smaller, which means that the spatially averaged value of the pressure received from the baffled circular piston will tend toward the pressure at a point on the transmitter axis. For large γ, the transmitter is getting smaller, which means that its energy output (for constant output pressure per the definition of D) is decreasing. For very large γ this reduces the average pressure on the front face of the receiving transducer to zero.

In the practical situation of predicting experimental results, D is noted to be proportional to the received signal magnitude. Because the received signal magnitude depends upon circuit electrical impedances, its absolute value is not relevant. When the calculated D and the experimental results are both separately normalized to unity, they should be identical. The normalized D values for reciprocal γs, then, will demonstrate reciprocity in magnitude as well as spatial variation.

The unfocused, circular plane piston effective radius, a_{eff}, is a parameter which takes into account sensitivity and phase variations over the transducer face and is used to match simple cw theory to the actual transducer beam pattern. It can be determined accurately from transducer axial point pressure extrema (maxima and minima) position measurements, z_m, using the known relation [2]:

$$a_{\text{eff}} = \left(z_m m\lambda + m^2\frac{\lambda^2}{4}\right)^{1/2} \quad (4)$$

where $m = 2n-1$ for maxima, $m = 2n$ for minima, $n = 1, 2, 3 \ldots$ and a_{eff} is calculated for each z_m. (Note that a slight error in the formulas for m given in [2] has been corrected here.) The average of all calculated a_{eff} values is taken as the effective radius. The more extrema present in the measurement results, the more accurate the resulting average a_{eff} value.

In order to observe the effect of the finite hydrophone diameter on the effective radius measurement, (2) is used. Fig. 2 shows the unfocused plane piston axial pressure measurement results for a 1 cm radius transducer and several finite dimension hydrophones. A large hydrophone diameter causes signal amplitude distortion and the phase

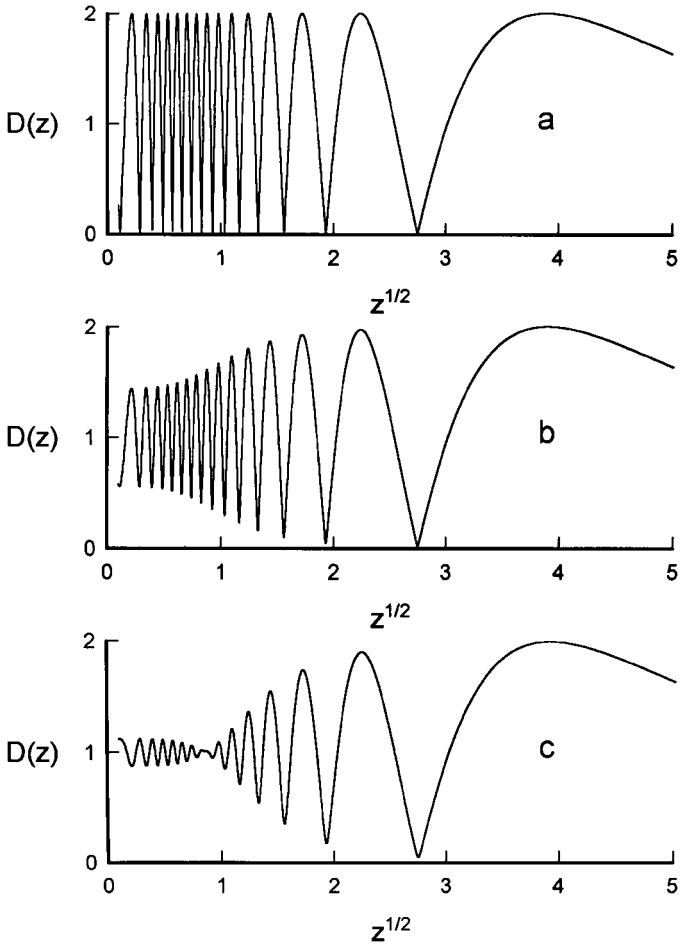

Fig. 2. Calculated axial pressure vs. $z^{1/2}$ for a 1 cm radius transducer with several hydrophones: (a) 0.02 mm diameter ($\gamma = 0.001$), (b) 0.5 mm diameter ($\gamma = 0.025$), and (c) 1 mm diameter ($\gamma = 0.050$) in water at 20°C. The square root of z was plotted to spread out the higher order extrema.

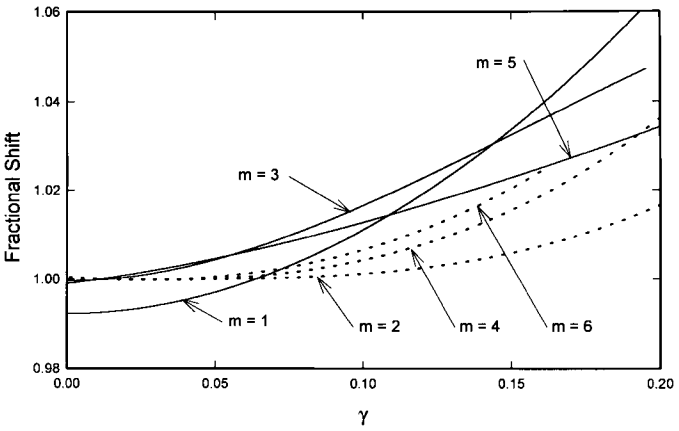

Fig. 3. Fractional shift of first six axial pressure extrema of an unfocused, circular piston measured with a circular hydrophone as a function of γ. The fractional shift is defined with respect to the unshifted values of (1). The odd m maxima demonstrate a larger change in lower order maxima at large γ, and the even m minima demonstrate a larger change in higher order maxima at large γ.

reversal of some extrema (maxima become minima and visa versa). The extrema at the shorter z values (higher order extrema, large m) are affected the most when γ increases. The lower order extrema (at larger z values) are least affected by large hydrophone diameter. However, any changes in z_m will affect the accuracy of the calculated average a_{eff} value using (4), so a pertinent question is, what exactly is the extremum axial position shift as a function of hydrophone diameter?

The calculation of the shift of the steady-state maximum or minimum axial positions with hydrophone diameter (or γ) is discussed in the Appendix and presented in Fig. 3. The lower order maxima have the largest shifts with increasing γ, and the higher order minima have the larger shifts with increasing γ.

At low values of γ (small hydrophones) only the lowest order maximum ($m = 1$) has an appreciable shift ($\sim$1%) in axial position from the point pressure lowest order maximum. This is shown in the Appendix to be due to water attenuation and the broadness of this peak.

III. Methods and Materials

Two unfocused, composite piezoelectric transducers of physical radii 0.938 and 1.25 cm were specially fabricated by Echo Ultrasound for this project. The transducers were suspended in a water tank ($\approx$20°C) mounted on a five axis (three translational, two rotational) computer controlled precision positioning system (Daedal Inc., Harrison City, PA) at UIUC, which has translational accuracy of about 2 μm.

Tone burst transmission was used to simulate steady-state (cw) conditions to avoid the deleterious effects of standing waves and multiple reflections in the tank. A 2.25-MHz, 15-cycle driving tone burst was generated by a Hewlett Packard (Santa Clara, CA) 8116A signal generator and amplified by an ENI 2100L 50 dB amplifier. The received signal was preamplified by a TEK 11A34 amplifier and displayed on a TEK 11401 digitizing oscilloscope at 1 mm axial distance increments. The received signals then were digitized and passed to a Tandy 4000 386 PC for processing. The pulse intensity integral, PII [5], was calculated over the entire received length of the tone burst in order to remove random noise and obtain the received pulse average intensity.

TABLE I
Effective Radius Results From the Measured z_m at 2.25 MHz.

a_{phys} cm	m	extremum	z_m cm	a_{eff} cm	avg a_{eff} cm
0.953	1	max	12.4	0.902	
	2	min	6.05	0.895	
	3	max	4.10	0.901	
	4	min	3.00	0.898	
	5	max	2.30	0.885	0.90
1.27	1	max	24.0	1.26	
	2	min	11.8	1.25	
	3	max	7.75	1.24	1.25

The axial acoustic pressure of each transducer was measured first using a Marconi 0.5 mm diameter bilaminar hydrophone. Then the two transducers were used in a pitch-catch measurement. Nonlinear propagation effects were avoided by maintaining the transmitter drive voltage low enough so that the second harmonic of the received signal was at least 30 dB below the fundamental.

IV. Results

Figs. 4(a) and (b) demonstrate the 0.5-mm-diameter hydrophone axial pulse average intensities at 2.25 MHz for the two Echo Ultrasound transducers. Only a limited number of low order extrema are present in these results. The larger transducer (1.25 cm physical radius) has the lower number of extrema and, potentially, the lower accuracy in the measured average a_{eff}. The $m = 1$ data was corrected back to point pressure using the fractional shift calculated for a 0.5-mm-diameter hydrophone measuring the extrema of a 0.90- or 1.25-cm-radius transducer. Table I presents the estimated effective radii, a_{eff}, for the measured extrema and the calculated average effective radii for the two transducers at 2.25 MHz.

Fig. 5 demonstrates the normalized result of the pitch-catch measurements using the two Echo Ultrasound transducers along with the normalized theoretical prediction of D corrected for water attenuation. The two normalized experimental measurements (with reciprocal γ values) do exhibit acoustic reciprocity within experimental uncertainty. At small z the normalized theoretical and experimental results do not agree. At large z there appears to be agreement between the two with a systematic error.

V. Discussion

Single crystal, unfocused plane piston transducers can have contributions from radial modes [6] that will lead

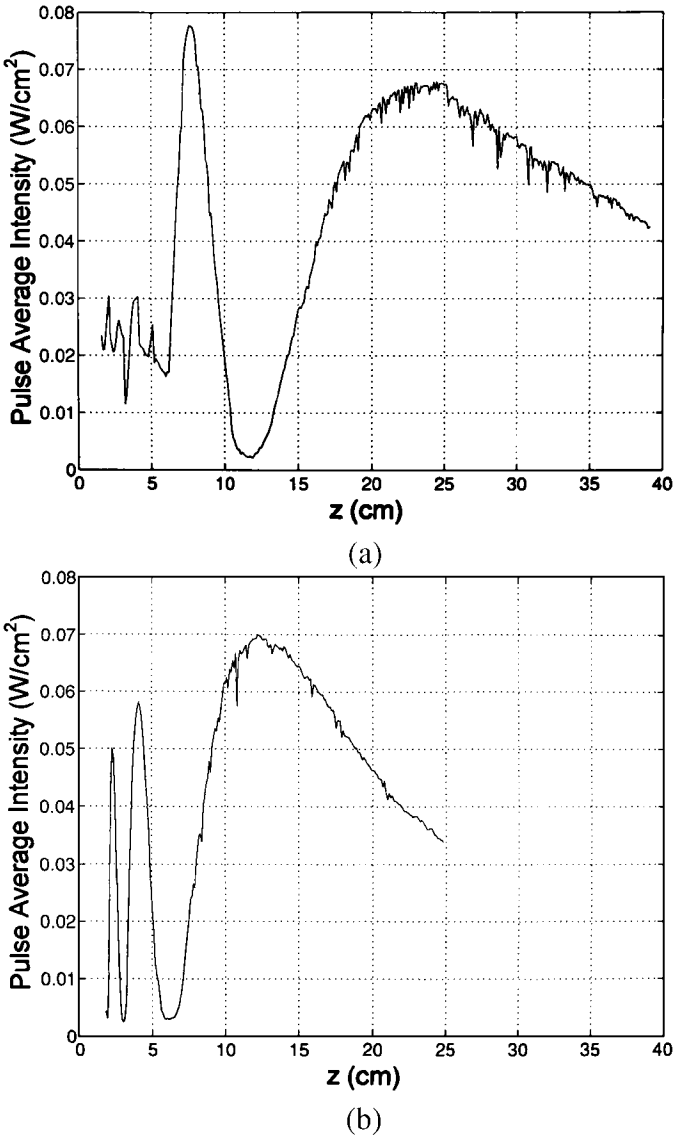

Fig. 4. Measured axial pulse average intensity at 2.25 MHz: (a) 1.27 cm radius transducer, and (b) 0.95 cm radius transducer.

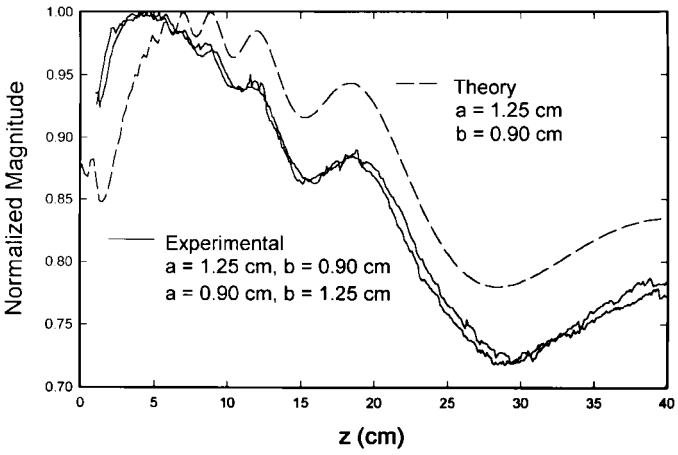

Fig. 5. Comparison of normalized theoretical and experimental results for pitch-catch co-axial measurements using the two Echo Ultrasound transducers. The two experimental curves obtained by switching transmitter and receiver functions exhibit acoustic reciprocity. Only one theoretical curve is shown because the normalized theoretical curves are identical.

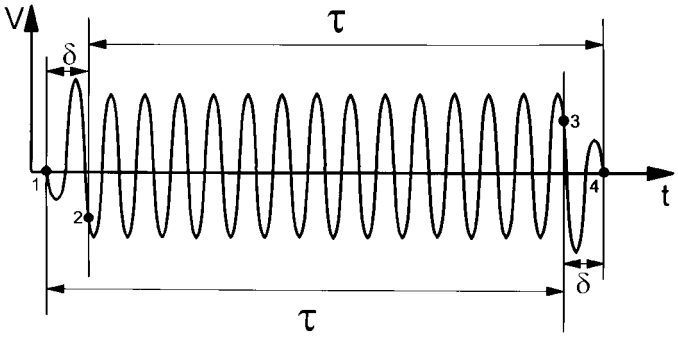

Fig. 6. Received tone burst signal demonstrating regions of transient diffraction at its leading edge (between points 1 and 2) and at its trailing edge (between points 3 and 4). The peak signal in the transient diffraction region is shown larger than the peak signal received in the steady-state region to demonstrate this improbable but possible circumstance. If the AIUM/NEMA pulse intensity integral is evaluated over an integral number of half cycles inside of the central steady-state diffraction region of the received tone burst signal, the cw intensity of the tone burst will be obtained.

to disagreement between measurement and theory. However, this will not occur with the composite piezoelectric transducers used here. The lack of agreement between experiment and theory for the two transducer pitch-catch measurement is due to the fact that the pulse intensity integral, which was used to analyze the received tone burst signals, is defined for short pulse radiation and the theory assumes cw conditions. Due to geometric propagation time delays, not all of the received tone burst signal is effectively a cw steady-state signal.

The received signal is "steady-state" when all portions of the receive transducer front surface in Fig. 1 are receiving signals from all portions of the transmit transducer front surface. At the leading and trailing edges of the received tone burst signal this condition is not satisfied as shown in Fig. 6. When the cophasal transmitter emits a tone burst, the face center of the receive transducer is the first region to receive a signal from the transmitter face center (point 1) and the receive face edge is the last region to receive a signal from the opposite transmit face edge (point 2). The time interval between points 1 and 2 is called here the transient diffraction duration and was described by Lord [7]. At the trailing edge of the received tone burst, a similar region of transient diffraction occurs between the points 3 (when the receive face center no longer receives signal from the transmit face center) and 4 (when the receive face edge no longer receives signal from the opposite transmit face edge). Between points 2 and 3 there exists a region of steady-state diffraction in which the signal amplitude is predictable from steady-state theory. All measurements must be made in this "steady-state" diffraction region to obtain "cw signals."

The transient diffraction duration $\delta(z)$ is equal to the time difference between the face center signals being received and the opposing edge signals being received and is

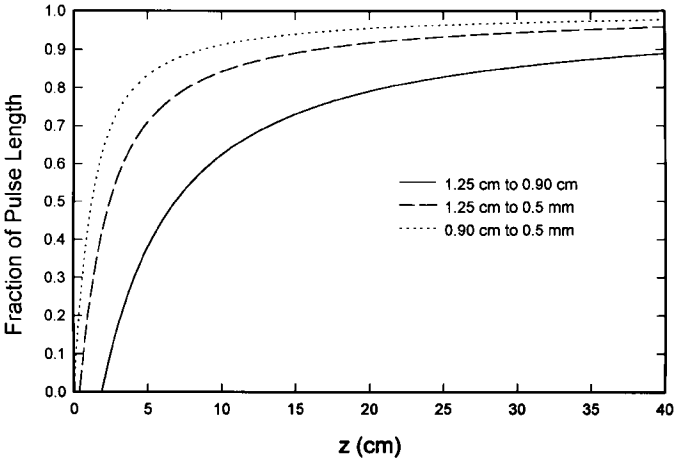

Fig. 7. Calculated steady-state fraction of the received tone burst length using (5) for the 15 cycle transmitted tone burst. Note that, even in the case of small diameter hydrophone reception, there is substantial transient diffraction at short distances from the transmitter.

given by:

$$\delta(z) = \frac{\sqrt{(a+b)^2 + z^2} - z}{c} \tag{5}$$

where c is the acoustic speed of the propagation medium. The transducer radii used in (5) must be their actual physical radii and not their effective radii. This is especially important when using membrane hydrophones whose effective radii are known to vary with frequency and angle [8].

The transmitted tone burst contains ε cycles with a total length $\tau = \varepsilon/f$, where f is the transmit frequency. The total length of the receive tone burst is $\tau + \delta(z)$ (Fig. 6) and the length of the steady-state diffraction region is $\tau - \delta(z)$. The fraction of the received tone burst length that is in steady-state diffraction is $(\tau - \delta(z))/(\tau + \delta(z))$. Fig. 7 demonstrates that, for the 1.25-cm-radius transducer transmitting to the 0.90-cm-radius transducer, the steady-state region of the received tone burst is substantial only at separations greater than 20 cm. At separations less than 5 cm, the experimental data were severely compromised (due to evaluation of the pulse intensity integral over the total length of the received pulse) resulting in the lack of agreement between experiment and theory. At separations less than 20 cm, the experimental data were moderately compromised, resulting in a change of magnitude of the short range signal that affected the normalization and caused the systematic error seen in Fig. 5.

It is interesting to note from Fig. 7 that even when the axial intensity of each transducer was measured using the 0.5-mm-diameter hydrophone, at separations less than 5 cm, there is substantial transient diffraction. This explains the lack of high order extrema in Figs. 4(a) and (b), which lowered the accuracy of the a_{eff} calculation. According to (5), the larger diameter receiving transducer measurement has more transient diffraction and should exhibit fewer extrema as demonstrated in Figs. 4(a) and (b).

When measuring the central "steady state" portion of the received tone burst, the pulse intensity integral is not a meaningful parameter. The maximum temporal average intensity should be used instead for the measurement of I_{SPTA} as specified in Section 5.4.18 of [5].

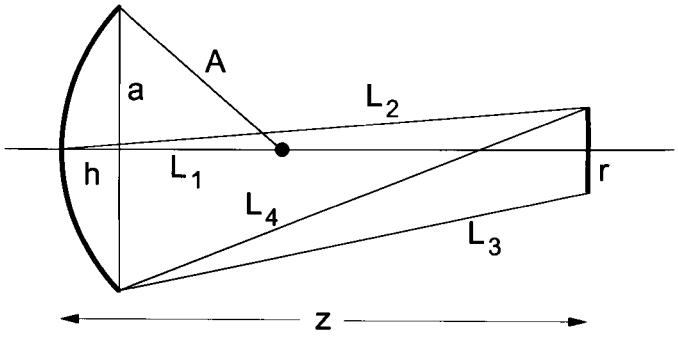

Fig. 8. Cross-sectional geometry of the co-axial measurement of a spherically focused transmitter by a flat receiver. The four extreme distances L_i from the transmitter to the receiver are shown.

VI. Focused Circular Piston

Although theoretical expressions exist for the axial point pressure of a spherically focused circular piston [9], [10], no theory exists for the diffraction correction D for co-axial hydrophone measurements of a spherically focused circular piston. Thus, the effect of the receiver diameter on the received spatially averaged pressure cannot be calculated, at present. Although spatial-averaging correction procedures have been worked out for some cases of interest [11], it is possible to estimate the transient diffraction duration using a simple geometric model to guide the analysis of experimental results.

Fig. 8 shows a cross-section view of the co-axial measurement geometry for a focused transmitter with a radius of curvature A. The focused transmitter has a circular aperture of radius a and the receiving flat circular piston has a radius r (actual physical radius). The distance notation of [9] is used with h given by [9]:

$$a^2 + h^2 = 2Ah.$$

Solving this quadratic equation for h, the physical solution obtained is:

$$h = A - \sqrt{A^2 - a^2}. \tag{6}$$

The four extreme distances in this measurement geometry are shown in Fig. 8. $L_1(z)$ is the axial distance between the centers of the two transducers:

$$L_1(z) = z, \tag{7}$$

$L_2(z)$ is the distance from the center of the transmitter to the edge of the receiver:

$$L_2(z) = \sqrt{r^2 + z^2}, \tag{8}$$

$L_3(z)$ is the shortest distance from the edge of the transmitter to the edge of the receiver:

$$L_3(z) = \sqrt{(z-h)^2 + (a-r)^2}, \tag{9}$$

and $L_4(z)$ is the longest distance from the edge of the transmitter to the edge of the receiver:

$$L_4(z) = \sqrt{(z-h)^2 + (a+r)^2}. \tag{10}$$

The calculation of the transient diffraction duration is straightforward for the common situation of small diameter hydrophones. Because $L_1(z)$ and $L_2(z)$ differ appreciably only when z is of order r, $L_2(z) \cong L_1(z)$. Throughout the full range of z, $L_4(z)$ is always greater than $L_3(z)$. From Fig. 8 for small r, it is evident that for z much less than A, $L_1(z)$ is shorter than either $L_3(z)$ or $L_4(z)$ and for z much greater than A, $L_1(z)$ is longer than either $L_3(z)$ or $L_4(z)$. Thus, there are three ranges of z to consider. At small z the maximum extreme distance difference is $L_4(z) - L_1(z)$. At large z the maximum extreme distance difference is $L_1(z) - L_3(z)$. And there is an intermediate range where the maximum extreme distance difference is $L_4(z) - L_3(z)$.

The transition distance z_L between the first two ranges is found by equating $L_4(z) - L_1(z)$ and $L_4(z) - L_3(z)$,

$$z_L = \frac{(a-r)^2 - h^2}{2h}. \tag{11}$$

And the transition distance z_H between the last two ranges is found by equating $L_1(z) - L_3(z)$ and $L_4(z) - L_3(z)$,

$$z_H = \frac{(a+r)^2 - h^2}{2h}. \tag{12}$$

Then, for the transient diffraction duration:

$$\delta(z) = \frac{\Delta L(z)}{c}, \tag{13}$$

where $\Delta L(z) = L_4(z) - L_1(z)$ when $z \le z_L$, $\Delta L(z) = L_4(z) - L_3(z)$ when $z_L \le z \le z_H$ and $\Delta L(z) = L_1(z) - L_3(z)$ when $z \ge z_H$.

The form of h in (6) is useful when A and a are used as transmitter focal parameters. It is also convenient to use the transmitter focal length F and f-number, fn, as parameters. For the degree of accuracy needed in this computation, F may be set equal to A. Substituting the definition of the f-number:

$$a = \frac{F}{2fn} \tag{14}$$

into (6) results in

$$h \cong F\left(1 - \sqrt{\frac{4fn^2 - 1}{4fn^2}}\right). \tag{15}$$

When using these results to analyze received tone-burst signals, it is necessary to know the transient diffraction duration in cycles of the transmitted frequency. This is obtained from (13) by dividing by the period of the frequency to obtain:

$$\delta T(z) = f\delta(z) \tag{16}$$

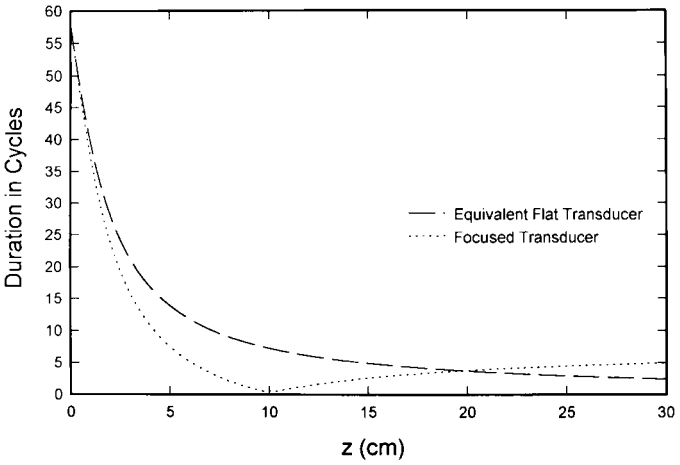

Fig. 9. Transient diffraction duration in cycles for a 3.5 MHz focused transmitter with a 10 cm radius of curvature and an f-number of 2 and its equivalent flat transducer, both measured by a 1.0 mm hydrophone. The minimum value for the focused transducer is 0.55 cycles compared to 7 cycles at the same distance for the equivalent flat transducer.

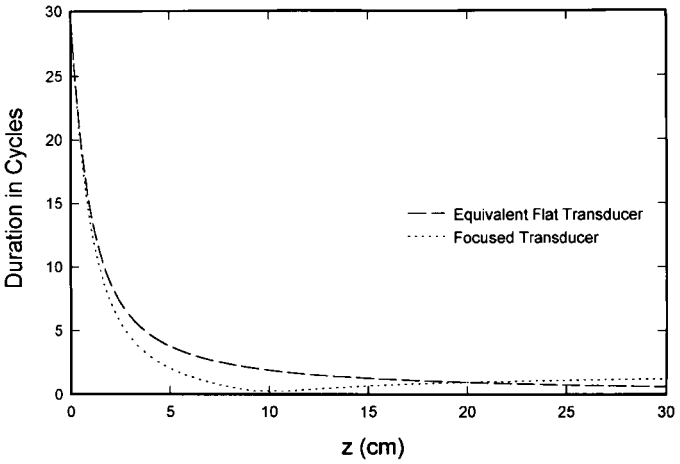

Fig. 10. Transient diffraction duration in cycles for a 3.5 MHz focused transmitter with a 10 cm radius of curvature and an f-number of 4 and its equivalent flat transducer, both measured by a 1.0 mm hydrophone. The minimum value for the focused transducer is 0.26 cycles compared to 1.77 cycles at the same distance for the equivalent flat transducer.

In commercial medical ultrasound equipment, focused transducers typically are designed with a $fn = 2$ focus for gray scale imaging and a weaker $fn = 4$ focus for range-gated Doppler signal acquisition [12]. For a 1.0-mm-diameter hydrophone co-axial measurement of a spherically focused circular 3.5-MHz-transducer with $A = 10$ cm, Fig. 9 shows $\delta T(z)$ when $fn = 2$ and Fig. 10 shows $\delta T(z)$ when $fn = 4$. Also plotted in these figures is the transient diffraction duration in cycles for the equivalent flat transducer [13], $L_{\text{flat}}(z)$, obtained by using (5) instead of (13) in (16). The transient diffraction duration is shorter for the focused transducer than the equivalent flat transducer, and this difference is greater the more strongly focused the transducer as seen in Figs. 9 and 10.

The plots in Figs. 9 and 10 exhibit shorter transient

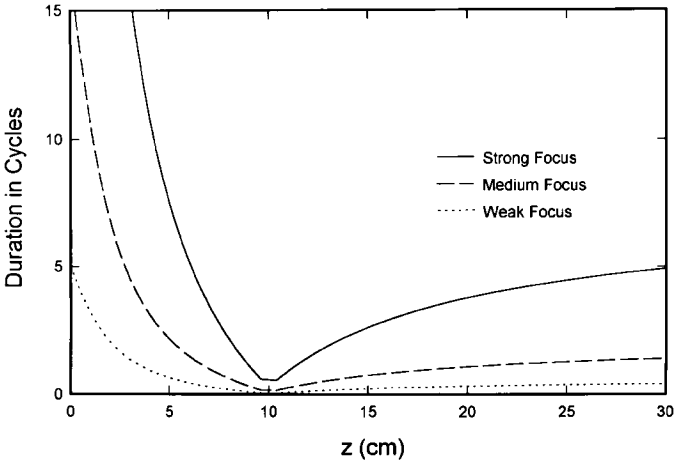

Fig. 11. Transient diffraction duration in cycles vs transmitter focal strength. The transmitter has a 10 cm radius of curvature and an f-number 2, and the hydrophone has a 1.0 mm diameter. The strong focus curve is for 3.5 MHz, the medium focus curve is for 1.0 MHz, and the weak focus curve is for 0.3 MHz. See text for details.

diffraction durations at close to moderate distances when the transducer is focused. At larger distances the equivalent flat transducer has the shorter transient diffraction duration. These distance variations in transient diffraction duration must be taken into account when analyzing received tone-burst signals for comparison to cw theoretical calculations. The transition distance where the focused and equivalent flat transducer curves cross is obtained by equating $L_1(z) - L_3(z)$ with $L_{\text{flat}}(z)$ yielding the cubic equation:

$$16hz^3 - (16a^2 + 16r^2 + 4h^2)z^2 + (16arh - 4h^3)z + 16a^2r^2 + h^4 - 8arh^2 = 0 \quad (17)$$

which can be solved using standard techniques [14]. The root that represents this physical problem is the large positive root.

It is also instructive to see how $\delta T(z)$ varies with the degree of transmitter focus. Focal strength has been defined as [13] weak focusing, $T/2 \leq A < \infty$; medium focusing, $T/2\pi \leq A < T/2$; and strong focusing, $A < T/2\pi$; where T is the transition distance of the equivalent flat transducer, a^2/λ. Again using the approximation that the focal distance F is equal to A and the definition of the f-number, for weak focusing the transmission frequency must be less than $8fn^2c/F$, for strong focusing the transmission frequency must be greater than $8\pi fn^2c/F$, and for medium focusing the transmission frequency is between these limits. Fig. 11 demonstrates $\delta T(z)$ for a 1.0-mm-diameter hydrophone co-axial measurement of a focused transducer with $A = 10$ cm, $fn = 2$ and the frequencies 3.5 MHz (strong focus), 1.0 MHz (medium focus), and 0.3 MHz (weak focus). The stronger the focus, the larger the transient diffraction duration in cycles, $\delta T(z)$. Note that the transient diffraction duration in seconds, $\delta(z)$, is independent of transmitter focal strength because it is independent of frequency.

VII. Conclusions

Geometric propagation time delays are known to cause transient diffraction regions at the leading and trailing edges of tone bursts. In any experiment designed to verify steady state cw theory, these transient diffraction regions must be avoided in the measurement.

When analyzing axial pressure data, the "effective" radii of flat, circular piston transducers may be accurately estimated using the diffraction correction D corrected for axial distance shifts due to broad pressure peaks and water attenuation.

Acknowledgment

Andras Gordon and Ronald Hileman of Echo Ultrasound produced the excellent composite piezoelectric flat, circular piston transducers used in this study.

Appendix

Axial distance shifts (from "point" positions) of the transmitting piston steady-state axial maxima or minima positions with receiving hydrophone diameter may be obtained by starting with the magnitude of the diffraction correction D (which is proportional to the received peak signal), adding a multiplicative exponential water attenuation term (with α/f^2 equal to 25.3 10^{-17} sec^2/cm at 20°C) [15], differentiating with respect to z and setting the result equal to zero.

Because the goal is to plot the shift in extremum position with γ, the approximate diffraction correction formula is not appropriate. The more complicated exact formula for $\gamma \leq 1$ must be used. After some algebra, the relation

$$(\cos(kz) - SR(k,z)) \cdot [-\alpha\cos(kz) + \alpha SR(k,z) - k\sin(kz) - kSRD(k,z)] = (\sin(kz) - SI(k,z)) \cdot [\alpha\sin(kz) - \alpha SI(k,z) - k\cos(kz) + kSID(k,z)] \quad (A1)$$

is obtained where,

$$SR(k,z) = \frac{2}{\pi\gamma^2}\int_{1-\gamma}^{1+\gamma}\sqrt{1-\left(\frac{1-\gamma^2+\xi^2}{2\xi}\right)^2} \times \cos\left(ka\sqrt{\xi^2+\left(\frac{z}{a}\right)^2}\right)d\xi, \quad (A2)$$

$$SI(k,z) = \frac{2}{\pi\gamma^2}\int_{1-\gamma}^{1+\gamma}\sqrt{1-\left(\frac{1-\gamma^2+\xi^2}{2\xi}\right)^2} \times \sin\left(ka\sqrt{\xi^2+\left(\frac{z}{a}\right)^2}\right)d\xi, \quad (A3)$$

$$SRD(k,z) = \frac{-2}{\pi\gamma^2}\int_{1-\gamma}^{1+\gamma}\frac{z\sqrt{1-\left(\frac{1-\gamma^2+\xi^2}{2\xi}\right)^2}}{\sqrt{\xi^2a^2+z^2}} \times \sin\left(ka\sqrt{\xi^2+\left(\frac{z}{a}\right)^2}\right)d\xi \text{ and} \quad (A4)$$

$$SID(k,z) = \frac{2}{\pi\gamma^2}\int_{1-\gamma}^{1+\gamma} \frac{z\sqrt{1-\left(\frac{1-\gamma^2+\xi^2}{2\xi}\right)^2}}{\sqrt{\xi^2a^2+z^2}} \times \cos\left(ka\sqrt{\xi^2+\left(\frac{z}{a}\right)^2}\right)d\xi. \quad \text{(A5)}$$

Using a numerical computer program (Mathcad, Mathsoft Corp., Cambridge, MA) the fractional shifts (with respect to "point" extremum values [4]) of the first three axial pressure maxima and minima were obtained and are presented in Fig. 3.

In order to verify the y axis intercept values of Fig. 3, where $\gamma = 0$, the relationship for the axial pressure of an unfocused circular piston radiator [4] was multiplied by the exponential water attenuation term, differentiated with respect to z and the result set equal to zero obtaining:

$$\alpha \sin\left[\frac{k}{2}\left(\sqrt{z^2+a^2}-z\right)\right] = \frac{k}{2}\left(\frac{z}{\sqrt{z^2+a^2}}-1\right) \times \cos\left[\frac{k}{2}\left(\sqrt{z^2+a^2}-z\right)\right]. \quad \text{(A6)}$$

The extremum values obtained with (A6) using the numerical computer program were identical to those calculated from (A1) with $\gamma = 0$. In both cases only the lowest order maximum ($m = 1$) had an appreciable fractional shift ($\sim 1\%$) in axial position. This fractional shift of the lowest order maximum varied monotonically with α becoming zero when $\alpha = 0$. Thus, this fractional shift is seen to be caused by the water attenuation and the broadness of this peak.

References

[1] P. Rogers and A. Van Buren, "An exact expression for the Lomel diffraction correction integral," *J. Acoust. Soc. Amer.*, vol. 55, pp. 724–728, 1974.

[2] A. Khimunin, "Ultrasonic propagation parameter measurements incorporating exact diffraction corrections," *Acustica*, vol. 39, pp. 87–95, 1978.

[3] K. Beissner, "Exact integral expression for the diffraction loss of a circular piston source," *Acustica*, vol. 49, pp. 212–217, 1981

[4] P. N. T. Wells, *Biomedical Ultrasonics*. London: Academic, 1977, p. 27.

[5] NEMA, "Acoustic output measurement standard for diagnostic ultrasound equipment," Rev. 1, Dec. 7, 1993, Standards Publication No. UD-2, National Electrical Manufacturers Association, Rosslyn, VA.

[6] C. Baboux, F. Lakestani, and M. Perdrix, "Theoretical and experimental study of the contribution of radial modes to the pulsed ultrasonic field radiated by a thick piezoelectric disk," *J. Acoust. Soc. Amer.*, vol. 75, pp. 1722–1731, 1984.

[7] A. Lord, Jr, "Changes in velocity of an elastic pulse owing to geometrical diffraction," *J. Acoust. Soc. Amer.*, vol. 19, pp. 163–169, 1966.

[8] R. Smith, "Are hydrophones of diameter 0.5 mm small enough to characterise diagnostic ultrasound equipment?" *Phys. Med. Biol.*, vol. 34, pp. 1593–1607, 1989.

[9] H. O'Neil, "Theory of focusing radiators," *J. Acoust. Soc. Amer.*, vol. 21, pp. 516–526, 1949.

[10] B. Lucas and T. Muir, "The field of a focusing source," *J. Acoust. Soc. Amer.*, vol. 72, pp. 1289–1296, 1982.

[11] B. Zequri and A. D. Bond, "The influence of waveform distortion on hydrophone spatial-averaging corrections—Theory and measurement," *J. Acoust. Soc. Amer.*, vol. 92, pp. 1809–1821, 1992.

[12] A. Goldstein, "Broadband transducers improve image quality," *Diagnostic Imaging*, vol. 15, pp. 89–93, 1993.

[13] G. Kossoff, "Analysis of focusing action of spherically curved transducers," *Ultrason. Med. Biol.*, vol. 5, pp. 359–365, 1979.

[14] M. Abramowitz and I. A. Stegun, *Handbook of Mathematical Functions*, Ninth Printing. New York: Dover, 1970, p. 17.

[15] J. Pinkerton, "The absorption of ultrasonic waves in liquids and its relation to molecular constitution," *Proc. R. Soc. Lond.*, vol. B62, pp. 129–141, 1949.

Albert Goldstein (M'72–SM'83) was born in New York, NY, on May 26, 1938. He received the B.S. degree in physics from the City College of New York, in 1960, and the Ph.D. degree in physics from the Massachusetts Institute of Technology, in 1965.

He is presently an associate professor of radiology at the Wayne State University School of Medicine. He was the Head of the Division of Medical Physics at Henry Ford Hospital from 1976 to 1984 and an assistant professor of radiology at the University of Kansas Medical Center from 1972 to 1976. He has been involved in the development of ultrasound imaging equipment and ultrasound quality assessment procedures.

Dr. Goldstein is a Fellow in the American Institute of Ultrasound in Medicine, the American College of Radiology, and the American Association of Physicists in Medicine. He is on the Editorial Board of the *Journal of Ultrasound in Medicine*.

William D. O'Brien, Jr. (S'64–M'71–SM'79–F'89) received B.S., M.S., and Ph.D. degrees in 1966, 1968, and 1970, from the University of Illinois, Urbana-Champaign.

From 1971 to 1975 he worked with the Bureau of Radiological Health (currently the Center for Devices and Radiological Health) of the U.S. Food and Drug Administration. Since 1975, he has been at the University of Illinois, where he is a Professor of Electrical and Computer Engineering and of Bioengineering, College of Engineering, and Professor of Bioengineering, College of Medicine, is the Director of the Bioacoustics Research Laboratory and is the Program Director of the NIH Radiation Biophysics and Bioengineering in Oncology Training Program. His research interests involve the many areas of ultrasound-tissue interaction, including spectroscopy, risk assessment, biological effects, tissue characterization, dosimetry, blood-flow measurements, acoustic microscopy and meat characterization for which he has published more than 170 papers.

Dr. O'Brien is Editor-in-Chief of the *IEEE Transactions on Ultrasonics, Ferroelectrics, and Frequency Control*. He is a Fellow of the Institute of Electrical and Electronics Engineers (IEEE), the Acoustical Society of America (ASA), and the American Institute of Ultrasound in Medicine (AIUM) and a Founding Fellow of the American Institute of Medical and Biological Engineering. He was recipient of the IEEE Centennial Medal (1984), the AIUM Presidential Recognition Awards (1985 and 1992), the AIUM/WFUMB Pioneer Award (1988), the IEEE Outstanding Student Branch Counselor Award (1989), and the AIUM Joseph H. Holmes Basic Science Pioneer Award (1993). He has been President (1982–1983) of the IEEE Sonics and Ultrasonics Group (currently the IEEE UFFC-Society), Co-Chairman of the 1981 IEEE Ultrasonic Symposium, and General Chairman of the 1988 IEEE Ultrasonics Symposium. He has also been President of the AIUM (1988–1991) and Treasurer of the World Federation for Ultrasound in Medicine and Biology (1991–1994).